Inorganic Chemistry

Article

pubs.acs.org/IC

Synthesis and Properties of the Cyano Complex of Oxo-Centered Triruthenium Core $[Ru_3(\mu_3\text{-}O)(\mu\text{-}CH_3COO)_6(pyridine)_2(CN)]$

Hua-Xin Zhang,*[,†] Yoichi Sasaki,*[,†] Yi Zhang,[†] Shen Ye,[†] Masatoshi Osawa,[†] Masaaki Abe,[‡] and Kohei Uosaki[§]

[†]Catalysis Research Center, Hokkaido University, Sapporo 001-0021, Japan

[‡]Department of Applied Chemistry, Graduate School of Engineering, Kyushu University, Nishi-ku, Fukuoka 819-0395, Japan

[§]Division of Chemistry, Graduate School of Science, Hokkaido University, Sapporo 060-0810, Japan

Supporting Information

ABSTRACT: The preparation and properties of a new cyano complex containing the $Ru_3(\mu_3\text{-}O)$ core, $[Ru_3(\mu_3\text{-}O)(\mu\text{-}CH_3COO)_6(py)_2(CN)]$ (**1**; py = pyridine), are reported. Complex **1** in CH_2Cl_2 showed intense absorption bands at 244, 334, and 662 nm, corresponding to a $\pi-\pi^*$ transition of the ligand, cluster-to-ligand charge transfer, and intracluster transitions, respectively. The cyclic voltammogram of **1** in 0.1 M $(n\text{-}Bu)_4NPF_6-CH_2Cl_2$ showed redox waves for the processes $Ru_3^{II,II,III}/Ru_3^{II,III,III}$, $Ru_3^{II,III,III}/Ru_3^{III,III,III}$, and $Ru_3^{III,III,III}/Ru_3^{III,III,IV}$ at $E_{1/2}$ = −1.49, −0.26, and +1.03 V vs Ag/AgCl, respectively. The first two redox potentials are more negative by ca. 0.2 V in comparison with the corresponding potentials of $[Ru_3(\mu_3\text{-}O)(\mu\text{-}CH_3COO)_6(py)_3]^+$. This is in sharp contrast to the positive shifts of the corresponding waves of $[Ru_3^{II,II,III}(\mu_3\text{-}O)(\mu\text{-}CH_3COO)_6(py)_2(CO)]$. Density functional theory (DFT) calculations of $[Ru_3^{II,III,III}(\mu_3\text{-}O)(\mu\text{-}CH_3COO)_6(py)_3]$, $[Ru_3^{II,III,III}(\mu_3\text{-}O)(\mu\text{-}CH_3COO)_6(py)_2(CN)]^-$, and $[Ru_3^{II,III,III}(\mu_3\text{-}O)(\mu\text{-}CH_3COO)_6(py)_2(CO)]$ showed that the positive charge of the ruthenium is delocalized over the triruthenium cores of the first two and is localized as $Ru^{II}(CO)\{Ru^{III}(py)\}_2$ in the CO complex. The calculations explain the difference in the π interactions of the two ligands with the triruthenium cores.

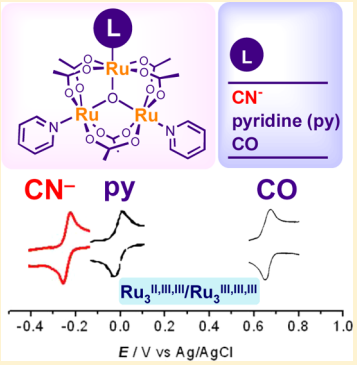

INTRODUCTION

Oxo−carboxylate-bridged di- and polynuclear metal complexes are known as important structural motifs not only in coordination chemistry but also in biological systems.[1−4] Di- and trinuclear units, $M_2(\mu\text{-}O)(\mu\text{-}RCOO)_n$ (n = 1, 2) and $M_3(\mu_3\text{-}O)(\mu\text{-}RCOO)_6$, are frequently found in many metal ions.[5−14] Among them, the ruthenium analogues have been the most extensively studied.[15−22] The kinetic stability of these structural cores in various oxidation states of Ru has been useful for detailed studies of these interesting structural units. The triruthenium complexes are especially attractive, since they can take a wide range of oxidation states from $Ru_3^{II,II,III}$ to $Ru_3^{III,IV,IV}$.[23−28] Recent extensive progress in the study of the triruthenium complexes is particularly noteworthy.[29−40] For example, dimerization and oligomerization of the triruthenium units by using bridging ligands such as pyrazine (pyz),[29−33,35−37] 4,4′-bipyridine (4,4′-bpy),[30,32] and diphosphine[39,40] led to the formation of Ru_3O-based mixed-valent dimers and oligomers. These new complexes brought new insights into the mixed-valence chemistry. New higher-nuclearity complexes based on the triruthenium core have also been reported.[41−47]

We have recently introduced the cyanide ion into the diruthenium unit $Ru_2(\mu\text{-}O)(\mu\text{-}CH_3COO)_2$[48] and found that the π-back-donation is less favorable. This is due to the poor π-donor properties of the dimeric unit as a result of usage of the relevant d electrons for the formation of the $Ru(d\pi)-O(p\pi)$ π-conjugated system. Therefore, the π-back-donation is unfavorable in the (μ-oxo)bis(μ-acetato)diruthenium complexes. A similar Ru−O π-system is also suggested for the triruthenium unit,[23,27] and the π-back-donation could be unfavorable. Nevertheless, the strong π-accepting ligand CO is known to form a stable complex with the triruthenium unit. The typical example is $[Ru_3^{II,III,III}(\mu_3\text{-}O)(\mu\text{-}CH_3COO)_6(py)_2(CO)]$ (py = pyridine),[23,49] where the significantly positive redox potential of the $Ru_3^{II,III,III}/Ru_3^{III,III,III}$ process indicates a characteristic feature of the π-back-donation to CO. It has been suggested that the charge localization within the triruthenium unit to form the $Ru^{II}(CO)\{Ru^{III}(py)\}_2$ electronic structure is useful in making the Ru−CO bond stable.[23] In fact, one-electron oxidation of the triruthenium complex destabilizes the Ru−CO bond to cause bond cleavage.[23] The corresponding CO complex has not been reported for the $Ru_2(\mu\text{-}O)(\mu\text{-}CH_3COO)_2$ unit. Charge localization may not effectively occur for the smaller $Ru_2(\mu\text{-}O)(\mu\text{-}CH_3COO)_2$ unit.

It is interesting to compare the coordination behavior of CN^- with that of CO toward the $Ru_3(\mu_3\text{-}O)(\mu\text{-}CH_3COO)_6$ core, which has a well conjugated π-system based on π-electron-rich Ru^{II} and/or Ru^{III} (d^6 and/or d^5, respectively).

Received: May 16, 2013
Published: December 5, 2013

   dx.doi.org/10.1021/ic4012197 | Inorg. Chem. 2014, 53, 1288−1294

Scheme 1. Synthesis of 1

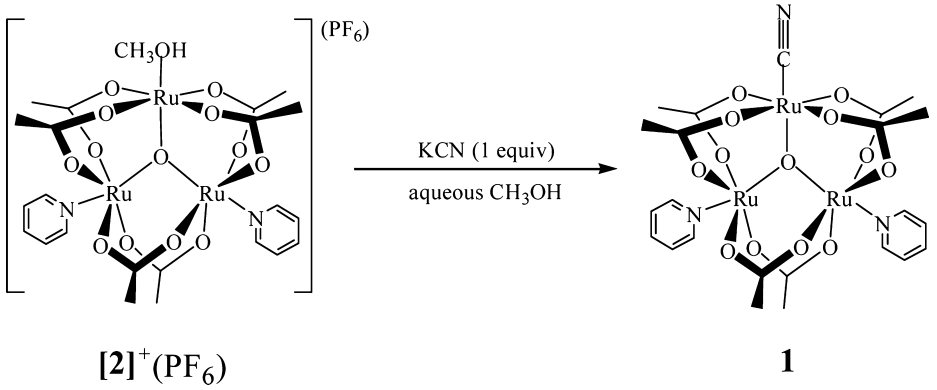

Cyanide ion is known as a weaker π-acceptor in comparison with CO.

This contribution presents the synthesis, properties, and computational study of a new cyano complex containing the $Ru_3(\mu_3\text{-}O)$ core, $[Ru_3(\mu_3\text{-}O)(\mu\text{-}CH_3COO)_6(py)_2(CN)]$ (**1**), and discusses the origin of the different coordination behaviors of CN^- and CO toward the $Ru_3(\mu_3\text{-}O)(\mu\text{-}CH_3COO)$ core.

RESULTS AND DISCUSSION

Synthesis and Characterization. The synthetic route to the new triruthenium cyano complex **1** is shown in Scheme 1. Facile ligand substitution for the solvent molecule of $[Ru_3(\mu_3\text{-}O)(\mu\text{-}CH_3COO)_6(py)_2(CH_3OH)](PF_6)$[23] ($[\mathbf{2}](PF_6)$) was applied for the preparation. Complex **1** was prepared by reacting $[\mathbf{2}]^+$ with an equimolar amount of KCN in a CH_3OH/H_2O mixed solvent at room temperature. The product was purified by column chromatography with silica gel.

Complex **1** was characterized by ^1H NMR and electrospray ionization mass spectrum (ESI-MS) as well as infrared spectroscopy and cyclic voltammetry (vide infra). The positive-ion ESI-MS showed a prominent signal at m/z 858.80, corresponding to the expected molecular ion peaks for **1**. The infrared spectrum showed the characteristic band of the cyano ligand at 2111 cm^{-1}, which is blue-shifted in comparison to that of the cyanide (2068 cm^{-1}) in KCN measured under the same conditions. The $\nu_{as}(COO^-)$ band is located at ca. 1607 and 1550 cm^{-1}, while the $\nu_s(COO^-)$ band is at 1420 cm^{-1}. The difference between $\nu_{as}(COO^-)$ and $\nu_s(COO^-)$ is greater than 130 cm^{-1}, indicating a bridging mode of the acetate groups.[23,50,51] Singlets due to the acetate methyl groups in the ^1H NMR spectrum of **1** (Figure S1, Supporting Information) are shifted significantly downfield (δ 11.01 (s, 12H), 5.98 (s, 6H)), while those of pyridine (δ 8.12 (t, 2H, py-4-H), 7.57 (q, 4H, py-3,5-H), 3.41 (d, 4H, py-2,6-H)) are shifted upfield in comparison with the corresponding signals of diamagnetic complexes.[23] It is known that the NMR signals of paramagnetic $Ru_3^{III,III,III}$ complexes of the $Ru_3(\mu_3\text{-}O)(\mu\text{-}CH_3COO)_6$ core show a rather mild shift from those of diamagnetic complexes, since the unpaired electron is delocalized over the whole area of the oxo-centered triruthenium core. The observed ^1H NMR spectrum of **1** is consistent with the $Ru_3^{III,III,III}$ oxidation state.

Electronic Absorption Spectroscopy. Figure 1 shows the UV−visible absorption spectrum of **1** in CH_2Cl_2, and Table 1 summarizes the spectral data. The triruthenium complexes $[Ru_3(\mu_3\text{-}O)(\mu\text{-}CH_3COO)_6(py)_2(L)]^+$ (L = py, *trans*-1,2-bis(4-pyridyl)ethylene (bpe), 1,2-bis(4-pyridyl)ethane (bpa), 4,4′-bpy, pyrazine)[23] generally show three main bands in their UV−vis absorption spectra: i.e., strong $\pi-\pi^*$ transitions of the ligand in the UV region, cluster-to-ligand charge transfer transitions (CLCT), and intracluster transitions in the longer wavelength region (>600 nm). As shown in Figure 1, complex **1** exhibits three bands at 244, 334, and 662 nm, which are assigned to the intraligand $\pi-\pi^*$, CLCT, and intracluster transitions, respectively.[39,51b] A theoretical study indicated that the lowest energy transitions remain practically as the intracluster type (vide infra). A blue shift of the intracluster transition band of **1** from those of $[Ru_3(\mu_3\text{-}O)(\mu\text{-}CH_3COO)_6(py)_2(L)]^+$ (692−694 nm) is ascribed to a stronger $d\pi(Ru)-p\pi(\mu\text{-}O)$ interaction within the Ru_3O core to give somewhat higher separations of the resulting molecular orbitals (see Theoretical Study of the Triruthenium Complexes of CN^- and CO).

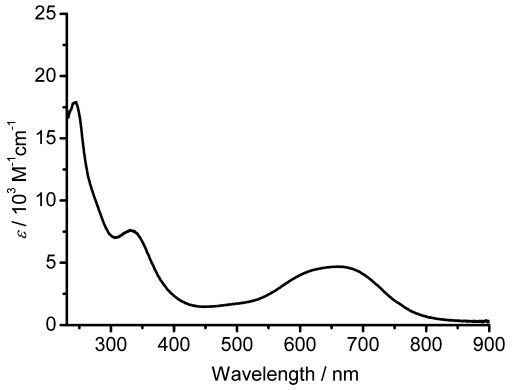

Figure 1. Electronic absorption spectrum of **1** in CH_2Cl_2.

Table 1. Absorption Spectral Data for 1 and Its Analogues

complex	λ_{max}, nm (ε, M^{-1} cm^{-1}) in CH_2Cl_2
1	662 (4700), 334 (7900), 244 (18500)
$[\mathbf{2}]^+$	689 (5440), 621 (4400), 240 (23640)
$[Ru_3(\mu_3\text{-}O)(\mu\text{-}CH_3COO)_6(py)_3]^+$ [a]	692 (5800), 240 (21000)

[a]Reference 23.

Redox Properties. Figure 2 shows the cyclic voltammogram of **1** in 0.1 M $(n\text{-}Bu)_4NPF_6-CH_2Cl_2$, and Table 2 summarizes the electrochemical data. Complex **1** shows three redox waves at $E_{1/2}$ = −1.49, −0.26, and +1.03 V vs Ag/AgCl, which are assigned to the processes $Ru_3^{II,II,III}/Ru_3^{II,III,III}$, $Ru_3^{II,III,III}/Ru_3^{III,III,III}$, and $Ru_3^{III,III,III}/Ru_3^{III,III,IV}$, respectively. Corresponding waves of $[Ru_3(\mu_3\text{-}O)(\mu\text{-}CH_3COO)_6(py)_3]^+$[23]

dx.doi.org/10.1021/ic4012197 | Inorg. Chem. 2014, 53, 1288−1294

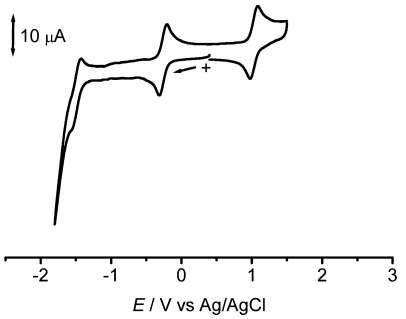

Figure 2. Cyclic voltammogram of **1** in 0.1 M (n-Bu_4)NPF_6–CH_2Cl_2: concentration of the complex, 0.3 mM; scan rate, 100 mV s^{-1}.

were observed at $E_{1/2}$ = −1.28, −0.01, and +1.01 V (Table 2), respectively. The first two redox potentials of **1** are appreciably more negative than those of the tris(pyridine) complex (the potential differences $\Delta E_{1/2}$ are 0.21 and 0.25 V, respectively, for the two negative waves). Thus, the lower oxidation states, $Ru_3^{II,II,III}$ and $Ru_3^{II,III,III}$, of the cyano complex **1** are destabilized significantly more than those of the corresponding py complex. This is, in part, due to the negative charge of the cyano ligand.

It is well-known that cyano complexes of d-electron-rich Fe(II), Ru(II), and Os(II) show significant solvent dependence in their various properties, including metal-centered redox potentials.[52] The solvent dependence has been interpreted in terms of the Lewis acid (solvent)–base (free nitrogen site of CN^- ligand) interaction. With a more acidic solvent, the redox potential appears at a more positive potential region, as the π-back-bonding is more favorable to make the metal center more difficult to oxidize. In a poorly acidic solvent such as CH_2Cl_2, the π-back-bonding is less favorable and even a simple π-donation is possible. π-Donor–acceptor properties of the metal–CN^- bond should also depend on the type of metal center; the π-back-donation is less significant with a lesser number of d electrons.[53] Thus, it is expected that the CN^- ligands coordinated to poor π-donating $Ru_2(\mu\text{-O})(\mu\text{-}CH_3COO)_2$ and $Ru_3(\mu_3\text{-O})(\mu\text{-}CH_3COO)_6$ (vide infra) cores are less favorable for π-back-donation.

The diruthenium unit $Ru_2(\mu\text{-O})(\mu\text{-}CH_3COO)_2$, despite the involvement of electron-rich Ru(II) and Ru(III) centers, is a π-deficient metal cluster core with dπ electrons being occupied by the Ru(dπ)–O(pπ) π-conjugated system. The redox potentials of $Ru_2^{II,II}/Ru_2^{II,III}$ and $Ru_2^{II,III}/Ru_2^{III,III}$ processes of the cyano complexes of the (μ-oxo)bis(μ-acetato)diruthenium core,[48] *trans*(*CN*,μ-*O*)-$[Ru_2^{III,III}(\mu\text{-O})(\mu\text{-}CH_3COO)_2(bpy)_2(CN)_2]$ (bpy = 2,2′-bipyridine) and its *cis* derivative, appear at considerably more negative potential regions in comparison with those of the pyridine diruthenium complexes $[Ru_2(\mu\text{-O})(\mu\text{-}CH_3COO)_2(N\text{–}N)_2(py)_2]^{2+}$, where N–N is $(py)_2$ or bpy.[20] The π-deficient nature of the dimeric core was supported by theoretical calculations, which showed that the Ru dπ electrons are occupied by the dπ(Ru)–pπ(μ-O) conjugation.

As a similar dπ–pπ conjugation system is also known for the $Ru_3(\mu_3\text{-O})(\mu\text{-}CH_3COO)_6$ core,[23] π-back-donation to the cyano ligand in **1** could be weaker than that normally expected for the M(II)–CN linkage in typical transition-metal–cyano complexes.

The situation is significantly different from that of the carbonyl ligand coordinated to the triruthenium core. The carbonyl complex $[Ru_3(\mu_3\text{-O})(\mu\text{-}CH_3COO)_6(py)_2(CO)]$[23] shows the redox wave of the $Ru_3^{II,III,III}/Ru_3^{III,III,III}$ process at +0.66 V vs Ag/AgCl, which is significantly more positive by 0.67 V in comparison with that of $[Ru_3(\mu_3\text{-O})(\mu\text{-}CH_3COO)_6(py)_3]^+$ (Table 2). The shift is interpreted on the basis of π-back-donation from the Ru center to CO.

The different behavior of CN^- and CO ligands coordinated to the triruthenium core is explained as follows. It has been suggested previously that the divalent charge of the $Ru_3^{II,III,III}$ oxidation state is localized at the Ru ion coordinated by CO and that this Ru ion is out of the dπ–pπ conjugation of the core.[23,49] Hence, the π-back-donation to CO becomes feasible by the charge localization within the Ru_3O core. For comparison, it is interesting to see the redox behavior of the isocyanide complex. Redox potentials of $[Ru_3(\mu_3\text{-O})(\mu\text{-}CH_3COO)_6(py)_2(CNXy)]$ (CNXy = 2,6-dimethylphenyl isocyanide)[54] appear to be more positive than the corresponding potentials of the pyridine complex $[Ru_3(\mu_3\text{-O})(\mu\text{-}CH_3COO)_6(py)_3]^+$,[23] but less significantly (Table 2). Thus, the isocyanide ligand appears to be a mild π-acceptor.

Infrared Spectroelectrochemistry. The ν(CN) value for complex **1** (oxidation state $Ru_3^{III,III,III}$) in KBr pellets is 2111 cm^{-1}. To further understand the redox behavior and the electronic structures of **1**, we carried out in situ infrared spectroelectrochemistry to monitor the vibration frequencies of the cyanide of the triruthenium unit in different oxidation states. Figure 3 shows the differential infrared spectra measured at different applied potentials for **1** in 0.1 M (n-$Bu)_4NPF_6$–CH_2Cl_2 solutions, with the reference spectrum recorded at +0.20 V, where the oxidation state of **1** is $Ru_3^{III,III,III}$. Table 3 summarizes the details of the band assignment.

The differential spectra measured at −0.50 and +1.50 V should correspond to the oxidation states of $Ru_3^{II,III,III}$ and $Ru_3^{III,III,IV}$, respectively. The downward band at 2111 cm^{-1} observed in both differential spectra corresponds to the disappearance of the $Ru_3^{III,III,III}$ oxidation state. The upward bands at 2072 and 2165 cm^{-1} are assigned to the $Ru_3^{II,III,III}$ and the $Ru_3^{III,III,IV}$ states, respectively. The increase in the ν(CN) values with an increase in the oxidation state is the general trend observed for various CN^- complexes.[55] The red shift of 39 cm^{-1} for the CN ligand was observed when $Ru_3^{III,III,III}$ (2111 cm^{-1}) was reduced to $Ru_3^{II,III,III}$ (2072 cm^{-1}) while a blue shift

Table 2. Electrochemical Data for 1 and Its Analogues

complex	$E_{1/2}$, V vs Ag/AgCl (ΔE_p, mV)		
	$Ru_3^{II,II,III}/Ru_3^{II,III,III}$	$Ru_3^{II,III,III}/Ru_3^{III,III,III}$	$Ru_3^{III,III,III}/Ru_3^{III,III,IV}$
1[a]	−1.49 (135)	−0.26 (105)	+1.03 (105)
$[Ru_3(\mu_3\text{-O})(\mu\text{-}CH_3COO)_6(py)_3]^+$ [b]	−1.28	−0.01	+1.01
$[Ru_3(\mu_3\text{-O})(\mu\text{-}CH_3COO)_6(py)_2(CO)]$[b]	−0.84	+0.66	+1.30
$[Ru_3(\mu_3\text{-O})(\mu\text{-}CH_3COO)_6(py)_2(CNXy)]$[c]	−0.96	+0.30	+1.15

[a]In 0.1 M (n-$Bu)_4NPF_6$–CH_2Cl_2. [b]In 0.1 M (n-$Bu)_4NPF_6$–CH_3CN. Reference 23. [c]In 0.1 M (n-$Bu)_4NPF_6$–CH_3CN. CNXy = 2,6-dimethylphenyl isocyanide. Reference 54.

dx.doi.org/10.1021/ic4012197 | *Inorg. Chem.* 2014, 53, 1288–1294

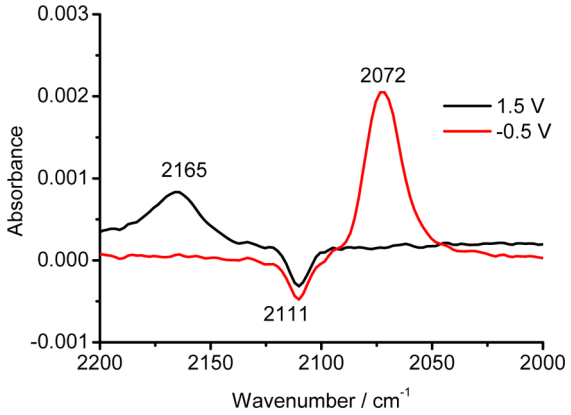

Figure 3. Potential-controlled infrared spectra of **1** in 0.1 M (n-Bu_4)NPF_6–CH_2Cl_2. Reference potential: 0.20 V.

Table 3. IR Bands of 1 in Different Oxidation States in 0.1 M (n-Bu_4)NPF_6–CH_2Cl_2

oxidation state of Ru_3O core	ν(CN), cm^{-1}
$Ru_3^{II,III,III}$	2072
$Ru_3^{III,III,III}$	2111
$Ru_3^{III,III,IV}$	2165

(54 cm^{-1}) was found for the oxidation of $Ru_3^{III,III,III}$ (2111 cm^{-1}) to $Ru_3^{III,III,IV}$ (2165 cm^{-1}). The smaller change in the wavenumber of the $Ru_3^{II,III,III}/Ru_3^{III,III,III}$ process (39 cm^{-1}) than that of $Ru_3^{III,III,III}/Ru_3^{III,III,IV}$ (54 cm^{-1}) may reveal two points: (i) In the $Ru_3^{II,III,III}/Ru_3^{III,III,III}$ process, the oxidation reaction did not occur on the CN-coordinated ruthenium, which indicated that the $Ru_3^{II,III,III}$ oxidation state of **1** was delocalized and no divalent charge was located on the CN-coordinated ruthenium. (ii) In the $Ru_3^{III,III,III}/Ru_3^{III,III,IV}$ process, the oxidation took place on the CN-coordinated ruthenium.

Theoretical Study of the Triruthenium Complexes of CN^- and CO. We have discussed the important difference in the roles of CN^- and CO coordinated to the $Ru_3(\mu_3\text{-O})$ core. While CO acts as a strong π-acceptor to the triruthenium core specifically in the oxidation state $Ru_3^{II,III,III}$, CN^- does not. The difference is explained in terms of the charge delocalization in the former and localization in the latter as $Ru^{II}(CO)\{Ru^{III}(py)\}_2$. To confirm the results, we have carried out the molecular orbital (MO) calculations on three $Ru_3^{II,III,III}$ complexes, $[Ru_3(\mu_3\text{-O})(\mu\text{-}CH_3COO)_6(py)_2(CN)]^-$, $[Ru_3(\mu_3\text{-O})(\mu\text{-}CH_3COO)_6(py)_2(CO)]$, and $[Ru_3(\mu_3\text{-O})(\mu\text{-}CH_3COO)_6(py)_3]$. The qualitative MO scheme has been suggested previously for oxo-centered triruthenium(III,III,III) complexes on the basis of the $d\pi(Ru)-p\pi(\mu_3\text{-O})$ interaction.[23,27,56] The outline of the scheme is as follows. When the z axis is taken perpendicularly to the $Ru_3(\mu_3\text{-O})$ plane and the x axis of each Ru atom in the direction of the Ru–(μ_3-O) bond, a π-type interaction among the three Ru d_{xz} and the μ_3-O p_z orbitals is suggested to give MOs in the frontier orbital region. The interaction gives one bonding, two nonbonding, and one antibonding orbital. The other $d\pi$ orbitals, d_{xy} and d_{yz}, of the three Ru ions should be found around the two $d\pi-p\pi$ nonbonding orbitals in energy. An unpaired electron in the $Ru_3^{III,III,III}$ oxidation state occupies one of these several nonbonding orbitals. The scheme may be applied to neighboring oxidation states of the triruthenium core. Thus, in the oxidation state of $Ru_3^{II,III,III}$, nonbonding orbitals are fully occupied and the antibonding orbital is the lowest unoccupied MO (LUMO).

First, we examined the charge distribution of the triruthenium core of the three $Ru_3^{II,III,III}$ complexes (Figure 4). Among the three complexes, the pattern of the charge

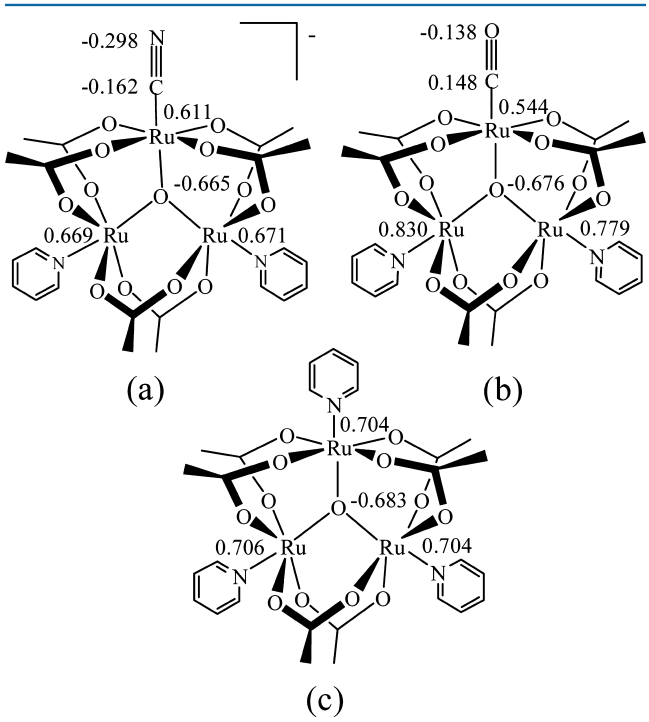

Figure 4. Charge distribution of complexes (a) $[Ru_3^{II,III,III}(\mu_3\text{-O})(\mu\text{-}CH_3COO)_6(py)_2(CN)]^-$, (b) $[Ru_3^{II,III,III}(\mu_3\text{-O})(\mu\text{-}CH_3COO)_6(py)_2(CO)]$, and (c) $[Ru_3^{II,III,III}(\mu_3\text{-O})(\mu\text{-}CH_3COO)_6(py)_3]$.

distribution of $[Ru_3(\mu_3\text{-O})(\mu\text{-}CH_3COO)_6(py)_2(CO)]$ is clearly different from the other two. The positive charge of the CO-coordinated Ru is significantly lower than those of the py-coordinated Ru (0.544 vs 0.779 and 0.830). The difference in the positive charges is much smaller for $[Ru_3(\mu_3\text{-O})(\mu\text{-}CH_3COO)_6(py)_2(CN)]^-$, where the CN-coordinated Ru has somewhat lower positive charge (0.611 vs 0.671 and 0.668). It is also noted that an appreciable amount of negative charge still remains on the carbon atom of the CN^- ligand. As expected, no appreciable difference in the charge distribution of the three Ru atoms is found for $[Ru_3(\mu_3\text{-O})(\mu\text{-}CH_3COO)_6(py)_3]$.

These results clearly support the previously suggested localized electronic state for the carbonyl complex: i.e., $Ru^{II}(CO)\{Ru^{III}(py)\}_2$.[23,49,57] The significantly smaller positive charge of the CO-coordinated Ru is favorable for the back-donation to CO. The structural localization of the CO complex indicates that the delocalized oxo-centered triruthenium core is not a good π-donor and requires the localization when a strongly π-accepting ligand coordinates. In contrast, the positive charge is practically delocalized over the triruthenium core in the case of the cyano complex. Thus, the $d\pi-p\pi$ interaction would be extended over the whole Ru_3O core by using Ru d_{xz} π electrons, and the core is π-deficient in the direction where CN^- approaches. Therefore, the back-donation in this direction is less favorable. The π-back-donations in the direction perpendicular to the Ru_3O plane may be operative but unlikely to be significant if they occurred. Structural localization would take place if the cyano ligand required the strong π-back-

dx.doi.org/10.1021/ic4012197 | Inorg. Chem. 2014, 53, 1288–1294

donation. The charge distribution of the Ru_3O-NO complex[58] $[Ru_3(\mu_3\text{-}O)(\mu\text{-}CH_3COO)_6(NH_3)_2(NO)]^+$ has been reported previously. A higher positive charge of the NO-coordinated Ru was noted that supports the electronic state of $Ru_3^{III,III,III}O\text{-}NO^0$ rather than $Ru_3^{II,III,III}O\text{-}NO^+$.

Since the metal cluster complexes in general can be electron-deficient, as the d electrons are used for the metal−metal bonding interactions or the dπ−pπ interactions as discussed above, the hitherto discussed different roles of π-type ligands such as CN^-, CO, NO, and isocyanide may be more commonly found in the metal cluster chemistry.

The energy levels and the components of the MOs near the frontier orbitals as obtained by the calculations for the ground-state molecular structures are given in Table 4, and the contour plots of the orbitals are shown in the Supporting Information (Figures S2−S4). First, the results on $[Ru_3(\mu_3\text{-}O)(\mu\text{-}CH_3COO)_6(py)_3]$ are discussed. The LUMO has a major contribution from three Ru and μ_3-O and is oriented perpendicularly to the Ru_3O plane (d_{xz}−p_z) (see the contour plot, Figure S2). The highest occupied MO (HOMO) and a few lower occupied orbitals are mainly composed of d_{xy} and d_{yz} orbitals. If we compare the qualitative MO scheme as described above to the calculated results in Table 4, despite the different oxidation states, the π^* orbital corresponds to the LUMO and the nonbonding orbitals to the HOMO and several lower orbitals. Since the HOMO is practically composed of the d orbitals that are oriented perpendicularly to those of LUMO, the HOMO−LUMO transition should be symmetrically forbidden. The nonbonding and bonding π orbitals resulting from the d_{xz}−p_z interaction should be mainly HOMO-5 and -6 and those in the deep bonding orbital region, respectively.

The Mülliken populations of the frontier orbitals of the $Ru_3^{II,III,III}$ cyano complex $[Ru_3(\mu_3\text{-}O)(\mu\text{-}CH_3COO)_6(py)_2(CN)]^-$ are similar to those of $[Ru_3(\mu_3\text{-}O)(\mu\text{-}CH_3COO)_6(py)_3]$. Here again the LUMO, which has a significant contribution from μ_3-O (24%), should correspond to the π^* orbital obtained from the d_{xz}−p_z interaction, and the HOMO is distributed perpendicularly to it. The contribution from the two different Ru sites (Ru−CN and Ru−py) has been calculated. While the LUMO receives more contribution from Ru(CN) (29%), the HOMO gets less (21%). Nevertheless, the difference in the contribution from the two different Ru atoms is not significant, and it is concluded that all three Ru atoms are involved in the dπ−pπ interaction. The Mülliken population of the CO complex is quite different from that of the CN^- complex. The LUMO again corresponds to the π^* orbital of the d_{xz}−p_z interaction but has only a small contribution (5%) from CO-coordinated Ru. It is thus concluded that the dπ−pπ interaction occurs mainly among two py-coordinated Ru atoms and μ_3-O. The result further supports the localized picture of the Ru_3O core in the CO complex: i.e., $Ru^{II}(CO)\{Ru^{III}(py)\}_2$ (vide supra).

The energy levels of the cyano complex are generally much higher than those of the other two $Ru_3^{II,III,III}$ complexes, due to the negative charge of the ligand CN^-. This, as well as the σ-donation from the CN^- ligand, primarily explains the destabilization of the $Ru_3^{II,III,III}$ state against oxidation.

CONCLUSIONS

We have introduced cyanide ion to the terminal site of the triruthenium core $Ru_3(\mu_3\text{-}O)(\mu\text{-}CH_3COO)_6$ to obtain $Ru_3(\mu_3\text{-}O)(\mu\text{-}CH_3COO)_6(py)_2(CN)$ (**1**). The negative shift of the redox potentials of the processes $Ru_3^{II,II,III}/Ru_3^{II,III,III}$ and $Ru_3^{II,III,III}/Ru_3^{III,III,III}$, in comparison with those of $[Ru_3(\mu_3\text{-}O)(\mu\text{-}CH_3COO)_6(py)_3]^+$, is partly explained in terms of the negative charge. This is in sharp contrast to the π-accepting character (back-bonding) of CO, as $[Ru_3(\mu_3\text{-}O)(\mu\text{-}CH_3COO)_6(py)_2(CO)]$ shows a significantly positive shift of the potential of the $Ru_3^{II,III,III}/Ru_3^{III,III,III}$ process. The difference has been interpreted in terms of the different π-acceptor properties of the two ligands when they coordinate to the mixed-valent $Ru_3^{II,III,III}$ core. The strong π-accepting ligand CO is stabilized by the charge localization of the core in the $Ru_3^{II,III,III}$ state, where the divalent state is localized to the CO-

Table 4. Composition of the Frontier Orbitals of the Complexes $[Ru_3(\mu_3\text{-}O)(\mu\text{-}CH_3COO)_6(py)_3]$, $[Ru_3(\mu_3\text{-}O)(\mu\text{-}CH_3COO)_6(py)_2(CN)]^-$, and $[Ru_3(\mu_3\text{-}O)(\mu\text{-}CH_3COO)_6(py)_2(CO)]$

$[Ru_3(\mu_3\text{-}O)(\mu\text{-}CH_3COO)_6(py)_3]$					
		component (%)			
MO	MO energy (eV)	Ru	μ-O	acetate	py
L+5	−0.39	0	0	1	99
L+4	−0.39	0	0	1	99
L+3	−0.84	16	4	1	79
L+2	−1.03	5	0	0	95
L+1	−1.03	5	0	0	95
LUMO	−2.46	55	20	3	22
HOMO	−4.15	76	0	24	0
H-1	−4.15	76	0	24	0
H-2	−4.35	86	0	12	1
H-3	−4.47	80	1	12	8
H-4	−4.47	80	1	12	8
H-5	−4.76	84	5	7	4
H-6	−4.76	84	5	7	5
$[Ru_3(\mu_3\text{-}O)(\mu\text{-}CH_3COO)_6(py)_2(CN)]^-$							
		component (%)					
MO	MO energy (eV)	Ru(CN)	Ru(py)	μ-O	CN	acetate	py
L+4	1.58	0	1	0	0	1	98
L+3	1.57	0	0	0	0	1	99
L+2	1.01	0	6	0	0	0	94
L+1	0.99	0	5	0	0	0	95
LUMO	−0.15	29	39	24	3	3	1
HOMO	−2	21	58	0	3	18	0
H-1	−2.01	45	32	0	0	23	0
H-2	−2.12	63	14	1	11	9	2
H-3	−2.27	24	55	0	5	15	1
H-4	−2.36	10	68	3	2	7	8
$[Ru_3(\mu_3\text{-}O)(\mu\text{-}CH_3COO)_6(py)_2(CO)]$							
		component (%)					
MO	MO energy (eV)	Ru(CO)	Ru(py)	μ-O	CO	acetate	py
L+5	−0.23	53	24	0	1	22	1
L+4	−0.67	0	1	0	0	1	98
L+3	−0.74	0	1	0	0	1	99
L+2	−1.19	0	3	0	0	0	97
L+1	−1.25	0	3	0	0	0	97
LUMO	−3.38	5	64	24	2	4	1
HOMO	−5	57	19	0	0	24	0
H-1	−5.09	1	71	0	0	28	0
H-2	−5.34	7	71	1	1	16	4
H-3	−5.4	1	79	0	0	18	1
H-4	−5.53	3	72	7	2	10	6

dx.doi.org/10.1021/ic4012197 | Inorg. Chem. 2014, 53, 1288−1294

bonded Ru. In contrast, the triruthenium core shows a delocalized structure in the cyano complex. The difference in the role of two ligands is further discussed with the aid of MO calculations. Further comparative studies on the coordination behavior of the two ligands to other metal clusters with metal−metal bonding interactions or dπ−pπ interactions are certainly of interest.

EXPERIMENTAL SECTION

Materials. All chemical reagents were commercially supplied and used without further purification unless otherwise stated. Silica gel (Wakogel C-300HG) was used for column chromatography. The CH_2Cl_2 solvent used for electrochemical measurements was distilled over CaH_2 under an Ar atmosphere. $[Ru_3(\mu_3\text{-}O)(\mu\text{-}CH_3COO)_6(py)_2(CH_3OH)](PF_6)$ ($[\mathbf{2}](PF_6)$)[23] was synthesized by using the reported methods.

$[Ru_3(\mu_3\text{-}O)(\mu\text{-}CH_3COO)_6(py)_2(CN)]\cdot CHCl_3$ (1·$CHCl_3$). To a solution of $[\mathbf{2}](PF_6)$ (100 mg, 0.10 mmol) in CH_3OH (50 mL) was added an aqueous solution (5 mL) of KCN (6.5 mg, 0.10 mmol) with stirring, and the mixture was stirred overnight at room temperature. After 12 h, the resultant solution was filtered, and the filtrate was evaporated to dryness by a rotary evaporator. The residue was dissolved in water (50 mL), and the aqueous solution was extracted with CH_2Cl_2 (30 mL × 3). The organic layer was evaporated to dryness, and the resultant blue solid was purified by column chromatography on silica gel with acetone as eluent. The second band, a major product which was eluted, was collected, and the solvent was removed by a rotary evaporator. Recrystallization of the residue from $CHCl_3$ gave a deep blue solid. Yield: 21 mg (25%). Anal. Calcd for $C_{23}H_{28}N_3O_{13}Ru_3\cdot CHCl_3$: C, 29.50; H, 2.99; N, 4.30. Found: C, 29.22; H, 3.01; N, 4.04. Positive ESI-MS (acetone): m/z 858.80 ($[M + H]^+$). Selected IR data (KBr pellet, cm^{-1}): 2111 m (CN^-), 1607 m ($\nu_{as}(COO^-)$), 1553 m ($\nu_{as}(COO^-)$), 1419 vs ($\nu_s(COO^-)$). ^1H NMR (CD_2Cl_2): δ 11.01 (s, 12H, CH_3COO^-), 8.12 (t, 2H, py 4-H), 7.63 (q, 4H, py 3,5-H), 5.98 (s, 6H, CH_3COO^-), 3.41 (d, 4H, py 2,6-H). UV−vis (CH_2Cl_2): λ_{max}/nm ($\varepsilon/M^{-1}\ cm^{-1}$) 662 (4700), 334 (7900), 244 (18500).

Safety Note. *Caution!* The cyanide salts are potentially hazardous. These chemicals should be handled with extreme caution in small quantities.

Physical Measurements. Ultraviolet and visible (UV−vis) absorption spectra were measured with a JASCO V-560 spectrophotometer. ^1H NMR spectra were obtained at 400 MHz with an EXC-400 NMR spectrometer. Infrared absorption spectra were recorded on a Bio-Rad FTS 60A/896 FT-IR spectrometer. The positive-ion ESI-MS measurements were performed on a JMS-T100LP mass spectrometer. Elemental analyses were carried out at the Center for Instrumental Analysis, Hokkaido University. Electrochemical measurements were carried out at room temperature in CH_2Cl_2 solutions containing 0.1 M $(n\text{-}Bu)_4NPF_6$ by using a potentiostat (EG&G, Model 263A) with a glassy-carbon working electrode. The potentials were recorded vs Ag/AgCl (saturated KCl solution) electrode. Pt mesh was used as a counter electrode.

The infrared spectroelectrochemistry was carried out on a Bio-Rad FTS 60A/896 FT-IR spectrometer equipped with a liquid-N_2-cooled HgCdTe detector. A homemade thin-layer IR spectroelectrochemical cell with a CaF_2 window was used for in situ IR and electrochemical measurements.[49] The incidence angle of the infrared beam was approximately 65°. A mirror-finish gold disk used as a working electrode was pushed against the CaF_2 window. The liquid layer between the electrode and the window was very thin, only about 1 μm, so that redox processes of solution species were expected to complete rapidly as soon as the electrode potential was changed. The potential was referenced to the Ag/AgCl (saturated KCl solution) electrode, and a Pt foil was used as the counter electrode. Each spectrum with a total of 512 interferograms with 4 cm^{-1} resolution was collected at each potential.

Theoretical Calculations. The theoretical calculations were carried out by density functional theory (DFT) methods with the B3LYP function by using the Gaussian 03 program.[59] The molecular models of the $Ru_3^{II,III,III}$ species $[Ru_3^{II,III,III}(\mu_3\text{-}O)(\mu\text{-}CH_3COO)_6(py)_2(CN)]^-$ and $[Ru_3^{II,III,III}(\mu_3\text{-}O)(\mu\text{-}CH_3COO)_6(py)_2(CO)]$ were constructed on the basis of the crystal structure data of the complex $[Ru_3^{II,III,III}(\mu_3\text{-}O)(\mu\text{-}CH_3CO_2)_6(mbpy^+)_2(CO)]^{2+}$ ($mbpy^+$ = *N*-methyl-4,4′-bipyridinium ion),[51b] whereas that of $[Ru_3^{II,III,III}(\mu_3\text{-}O)(\mu\text{-}CH_3COO)_6(py)_3]$ was referenced to the crystal structure of $[Ru_3^{II,III,III}(\mu_3\text{-}O)(\mu\text{-}CH_3CO_2)_6(py)_3]$.[60] All of the models were optimized to the minimum-energy point.

ASSOCIATED CONTENT

Supporting Information

Figures giving the ^1H NMR spectrum of complex **1** and contour plots of MOs of $[Ru_3(\mu_3\text{-}O)(\mu\text{-}CH_3COO)_6(py)_3]$, $[Ru_3(\mu_3\text{-}O)(\mu\text{-}CH_3COO)_6(py)_2(CN)]^-$, and $[Ru_3(\mu_3\text{-}O)(\mu\text{-}CH_3COO)_6(py)_2(CO)]$. This material is available free of charge via the Internet at http://pubs.acs.org.

AUTHOR INFORMATION

Corresponding Authors

*E-mail for H.-X.Z.: zhanghx@gxu.edu.cn.

*E-mail for Y.S.: ysasaki@sci.hokudai.ac.jp.

Notes

The authors declare no competing financial interest.

ACKNOWLEDGMENTS

This work was partially supported by a JSPS KAKENHI Grant (No. 24550143) and a Grant-in-Aid for Scientific Research on Innovative Areas "Coordination Programming" (Area 2107, Nos. 24108701 and 24108730) from the Ministry of Education, Culture, Sports, Science and Technology of Japan. H.-X.Z. is grateful to the Japan Society for the Promotion of Science for a postdoctoral fellowship (P05123). M.A. and S.Y. also gratefully acknowledge financial support from the Cooperative Research Program of the Catalysis Research Center, Hokkaido University (No. 12A0007).

REFERENCES

(1) (a) Lippard, S. J. *Angew. Chem., Int. Ed.* **1988**, *27*, 344−361. (b) Tinberg, C. E.; Lippard, S. J. *Acc. Chem. Res.* **2011**, *44*, 280−288.
(2) (a) Que, L., Jr.; Dong, Y. *Acc. Chem. Res.* **1996**, *29*, 190−196. (b) Vu, V. V.; Makris, T. M.; Lipscomb, J. D.; Que, L., Jr. *J. Am. Chem. Soc.* **2011**, *133*, 6938−6941.
(3) Wieghardt, K. *Angew. Chem.* **1989**, *101*, 1179; *Angew. Chem., Int. Ed.* **1989**, *28*, 1153−1172.
(4) Manchanda, R.; Brudvig, G. W.; Crabtree, R. H. *Coord. Chem. Rev.* **1995**, *144*, 1−38.
(5) Cannon, R. D.; White, R. P. *Prog. Inorg. Chem.* **1988**, *36*, 195−298.
(6) Houston, J. R.; Olmstead, M. M.; Casey, W. H. *Inorg. Chem.* **2006**, *45*, 7799−7805.
(7) Nakata, K.; Nagasawa, A.; Sasaki, Y.; Ito, T. *Chem. Lett.* **1989**, 753−756.
(8) Georgopoulou, A. N.; Sanakis, Y.; Boudalis, A. K. *Dalton Trans.* **2011**, *40*, 6371−6374.
(9) Figuerola, A.; Tangoulis, V.; Ribas, J.; Hartl, H.; Bruldgam, I.; Maestro, M.; Diaz, C. *Inorg. Chem.* **2007**, *46*, 11017−11024.
(10) Kurtz, D. M., Jr. *Chem. Rev.* **1990**, *90*, 585−606.
(11) Tshuva, E. Y.; Lippard, S. J. *Chem. Rev.* **2004**, *104*, 987−1012.
(12) Norman, R. E.; Yan, S.; Que, L., Jr.; Backes, G.; Ling, J.; Sanders-Loehr, J.; Zhang, J. H.; O'Connor, C. J. *J. Am. Chem. Soc.* **1990**, *112*, 1554−1562.
(13) Pal, S.; Gohdes, J. W.; Wilisch, W. C. A.; Armstrong, W. H. *Inorg. Chem.* **1992**, *31*, 713−716.

(14) Sugimoto, H.; Kitayama, K.; Ashikari, K.; Matsunami, C.; Ueda, N.; Umakoshi, K.; Hosokoshi, Y.; Sasaki, Y.; Itoh, S. *Inorg. Chem.* **2011**, *50*, 9014−9023.
(15) Cotton, F. A.; Norman, J. G.; Spencer, A.; Wilkinson, G. *J. Chem. Soc., Chem. Commun.* **1971**, 967−968.
(16) Spencer, A.; Wilkinson, G. *J. Chem. Soc., Dalton Trans.* **1972**, 1570−1577.
(17) Spencer, A.; Wilkinson, G. *J. Chem. Soc., Dalton Trans.* **1974**, 786−792.
(18) Cotton, F. A.; Norman, J. G., Jr. *Inorg. Chim. Acta* **1972**, *6*, 411−419.
(19) Sasaki, Y.; Nagasawa, A.; Tokiwa-Yamamoto, A.; Ito, T. *Inorg. Chim. Acta* **1993**, *212*, 175−182.
(20) Sasaki, Y.; Suzuki, M.; Nagasawa, A.; Tokiwa, A.; Ebihara, M.; Yamaguchi, T.; Kabuto, C.; Ochi, T.; Ito, T. *Inorg. Chem.* **1991**, *30*, 4903−4908.
(21) Fukumoto, T.; Kikuchi, A.; Umakoshi, K.; Sasaki, Y. *Inorg. Chim. Acta* **1998**, *283*, 151−159.
(22) Neubold, P.; Wieghardt, K.; Nuber, B.; Weiss, J. *Inorg. Chem.* **1989**, *28*, 459−467.
(23) Baumann, J. A.; Salmon, D. J.; Wilson, S. T.; Meyer, T. J. *Inorg. Chem.* **1978**, *17*, 3342−3350.
(24) Toma, H. E.; Araki, K.; Alexiou, A. D. P.; Nikolaou, S.; Dovidauskas, S. *Coord. Chem. Rev.* **2001**, *219*−*221*, 187−234.
(25) Toma, H. E.; Alexiou, A. D. P.; Formiga, A. L. B.; Nakamura, M.; Dovidauskas, S.; Eberlin, M. N.; Tomazela, D. M. *Inorg. Chim. Acta* **2005**, *358*, 2891−2899.
(26) Breedlove, B. K.; Yamaguchi, T.; Ito, T.; Londergan, C. H.; Kubiak, C. P. In *Comprehensive Coordination Chemistry II: from Biology to Nanotechnology*; McCleverty, J. A., Meyer, T. J., Eds.; Elsevier: Oxford, U.K., 2004; Vol. 2, p 717.
(27) Sasaki, Y.; Abe, M. *Chem. Rec.* **2004**, *4*, 279−290.
(28) (a) Inatomi, A.; Abe, M.; Hisaeda, Y. *Eur. J. Inorg. Chem.* **2009**, 4830−4836. (b) Chen, Z.-N.; Dai, F.-R. *Struct. Bonding (Berlin)* **2009**, *133*, 93−120.
(29) Wilson, S. T.; Bondurant, R. F.; Meyer, T. J.; Salmon, D. J. *J. Am. Chem. Soc.* **1975**, *97*, 2285−2287.
(30) Baumann, J. A.; Salmon, D. J.; Wilson, S. T.; Meyer, T. J. *Inorg. Chem.* **1979**, *18*, 2472−2479.
(31) Ito, T.; Hamaguchi, T.; Nagino, H.; Yamaguchi, T.; Washington, J.; Kubiak, C. P. *Science* **1997**, *277*, 660−663.
(32) Ito, T.; Hamaguchi, T.; Nagino, H.; Yamaguchi, T.; Kido, H.; Zavarine, I. S.; Richmond, T.; Washington, J.; Kubiak, C. P. *J. Am. Chem. Soc.* **1999**, *121*, 4625−4632.
(33) Ito, T.; Imai, N.; Yamaguchi, T.; Hamaguchi, T.; Londergan, C. H.; Kubiak, C. P. *Angew. Chem., Int. Ed.* **2004**, *43*, 1376−1381.
(34) Goeltz, J. C.; Kubiak, C. P. *J. Am. Chem. Soc.* **2010**, *132*, 17390−17392.
(35) Salsman, J. C.; Kubiak, C. P. *J. Am. Chem. Soc.* **2005**, *127*, 2382−2383.
(36) Salsman, J. C.; Ronco, S.; Londergan, C. H.; Kubiak, C. P. *Inorg. Chem.* **2006**, *45*, 547−554.
(37) Ohtsu, H.; Fujiwara, N.; Yamaguchi, T. *Inorg. Chem.* **2011**, *50*, 7382−7384.
(38) Ohtsu, H.; Kitazume, J.; Yamaguchi, T. *Dalton Trans.* **2011**, *40*, 7502−7504.
(39) Chen, J.-L.; Zhang, L.-Y.; Chen, Z.-N.; Gao, L.-B.; Abe, M.; Sasaki, Y. *Inorg. Chem.* **2004**, *43*, 1481−1490.
(40) Chen, J.-L.; Zhang, L.-Y.; Shi, L.-X.; Ye, H.-Y.; Chen, Z.-N. *Inorg. Chim. Acta* **2006**, *359*, 1531−1540.
(41) Dai, F.-R.; Chen, J.-L.; Ye, H.-Y.; Zhang, L.-Y.; Chen, Z.-N. *Dalton Trans.* **2008**, 1492−1502.
(42) Baumann, J. A.; Wilson, S. T.; Salmon, D. J.; Hood, P. L.; Meyer, T. J. *J. Am. Chem. Soc.* **1979**, *101*, 2916−2920.
(43) Abe, M.; Inatomi, A.; Hisaeda, Y. *Dalton Trans.* **2011**, *40*, 2289−2298.
(44) Hamaguchi, T.; Nagino, H.; Hoki, K.; Kido, H.; Yamaguchi, T.; Breedlove, B. K.; Ito, T. *Bull. Chem. Soc. Jpn.* **2005**, *78*, 591.
(45) Kido, H.; Nagino, H.; Ito, T. *Chem. Lett.* **1996**, 745−746.
(46) Nikolaou, S.; Toma, H. E. *Eur. J. Inorg. Chem.* **2008**, 2266−2271.
(47) Lear, B. J.; Kubiak, C. P. *Inorg. Chem.* **2006**, *45*, 7041−7043.
(48) Zhang, H.-X.; Tsuge, K.; Sasaki, Y.; Osawa, M.; Abe, M. *Eur. J. Inorg. Chem.* **2011**, 5132−5143.
(49) Ye, S.; Akutagawa, H.; Uosaki, K.; Sasaki, Y. *Inorg. Chem.* **1995**, *34*, 4527−4528.
(50) Cotton, F. A.; Wilkinson, G. *Advanced Inorganic Chemistry*, 5th ed.; Wiley: New York, 1988; p 253.
(51) (a) Ohto, A.; Tokiwa-Yamamoto, A.; Abe, M.; Ito, T.; Sasaki, Y.; Umakoshi, K.; Cannon, R. D. *Chem. Lett.* **1995**, 97−98. (b) Abe, M.; Sasaki, Y.; Yamada, Y.; Tsukahara, K.; Yano, S.; Yamaguchi, T.; Tominaga, M.; Taniguchi, I.; Ito, T. *Inorg. Chem.* **1996**, *35*, 6724−6734.
(52) (a) Posse, M. E. G.; Katz, N. E.; Baraldo, L. M.; Polonuer, D. D.; Colombano, C. G.; Olabe, J. A.; Garcia, M. E.; Nestor, P.; Diego, M. B. *Inorg. Chem.* **1995**, *34*, 1830−1835. (b) Toma, H.; Takasugi, M. *J. Sol. Chem.* **1983**, *12*, 547−561. (c) Toma, H.; Takasugi, M. *J. Sol. Chem.* **1989**, *18*, 575−583. (d) Bignozzi, C. A.; Chiorboli, C.; Indelli, M. T.; Rampi Scandola, M. A.; Varani, G.; Scandola, F. *J. Am. Chem. Soc.* **1986**, *108*, 7872−7873.
(53) Nelson, K. J.; Giles, I. D.; Shum, W. W.; Arif, A. M.; Miller, J. S. *Angew. Chem., Int. Ed.* **2005**, *44*, 3129−3132.
(54) Ota, K.; Sasaki, H.; Matsui, T.; Hamaguchi, T.; Yamaguchi, T.; Ito, T.; Kido, H.; Kubiak, C. P. *Inorg. Chem.* **1999**, *38*, 4070−4078.
(55) Kettle, S. F. A.; Diana, E.; Baccaleri, E.; Stanghellini, P. L. *Inorg. Chem.* **2007**, *46*, 2409−2416.
(56) Abe, M.; Sasaki, Y.; Yamada, Y.; Tsukahara, K.; Yano, S.; Ito, T. *Inorg. Chem.* **1995**, *34*, 4490−4498.
(57) Zhou, W.; Ye, S.; Abe, M.; Nishida, T.; Uosaki, K.; Osawa, M.; Sasaki, Y. *Chem. Eur. J.* **2005**, *11*, 5040−5054.
(58) Toma, H. E.; Alexiou, A. D. P.; Dovidauskas, S. *Eur. J. Inorg. Chem.* **2002**, 3010−3017.
(59) Frisch, M. J.; Trucks, G. W.; Schlegel, H. B.; Scuseria, G. E.; Robb, M. A.; Cheeseman, J. R.; Montgomery, J. A., Jr.; Vreven, T.; Kudin, K. N.; Burant, J. C.; Millam, J. M.; Iyengar, S. S.; Tomasi, J.; Barone, V.; Mennucci, B.; Cossi, M.; Scalmani, G.; Rega, N.; Petersson, G. A.; Nakatsuji, H.; Hada, M.; Ehara, M.; Toyota, K.; Fukuda, R.; Hasegawa, J.; Ishida, M.; Nakajima, T.; Honda, Y.; Kitao, O.; Nakai, H.; Klene, M.; Li, X.; Knox, J. E.; Hratchian, H. P.; Cross, J. B.; Bakken, V.; Adamo, C.; Jaramillo, J.; Gomperts, R.; Stratmann, R. E.; Yazyev, O.; Austin, A. J.; Cammi, R.; Pomelli, C.; Ochterski, J. W.; Ayala, P. Y.; Morokuma, K.; Voth, G. A.; Salvador, P.; Dannenberg, J. J.; Zakrzewski, V. G.; Dapprich, S.; Daniels, A. D.; Strain, M. C.; Farkas, O.; Malick, D. K.; Rabuck, A. D.; Raghavachari, K.; Foresman, J. B.; Ortiz, J. V.; Cui, Q.; Baboul, A. G.; Clifford, S.; Cioslowski, J.; Stefanov, B. B.; Liu, G.; Liashenko, A.; Piskorz, P.; Komaromi, I.; Martin, R. L.; Fox, D. J.; Keith, T.; Al-Laham, M. A.; Peng, C. Y.; Nanayakkara, A.; Challacombe, M.; Gill, P. M. W.; Johnson, B.; Chen, W.; Wong, M. W.; Gonzalez, C.; Pople, J. A. *Gaussian 03, revision D.02*; Gaussian, Inc., Wallingford, CT, 2004.
(60) Marr, S. B.; Carvel, R. O.; Richens, D. T.; Lee, H. J.; Lane, M.; Stavropoulos, P. *Inorg. Chem.* **2000**, *39*, 4630−4638.

■ NOTE ADDED AFTER ASAP PUBLICATION

This paper was published on the Web on December 5, 2013. The original version of this paper has been revised in light of concerns raised by a reader. The manuscript has been revised to avoid decisive expression on π-donation from the cyano ligand and also to weaken relevant statements. The new version has changes to the Table of Contents and Abstract graphics, Synopsis, Abstract, sections of the Results and Discussion, and Supporting Information. The corrected version was reposted on January 24, 2014.